Synthesis and Characterization of Poly(vinylidene fluoride)-*g*-sulfonated Polystyrene Graft Copolymers for Proton Exchange Membrane

Zhicheng Zhang,[⊥,†] Elena Chalkova,[‡] Mark Fedkin,[‡] Chunmei Wang,[‡] Serguei N. Lvov,[‡,§] Sridhar Komarneni,[∥] and T. C. Mike Chung*[,†]

Department of Materials Science and Engineering, The Pennsylvania State University, University Park, Pennsylvania 16802, The Energy Institute, The Pennsylvania State University, University Park, Pennsylvania 16802, Department of Energy and Geo-Environmental Engineering, The Pennsylvania State University, University Park, Pennsylvania 16802, and Department of Crop and Soil Sciences, The Pennsylvania State University, University Park, Pennsylvania 16802

Received June 6, 2008; Revised Manuscript Received October 8, 2008

ABSTRACT: A series of poly(vinylidene fluoride)-*g*-sulfonated polystyrene (PVDF-g-SPS) graft copolymers were systematically synthesized and examined with the focus of understanding how the polymer microstructure (backbone molecular weight, graft density, graft length, sulfonic acid concentration, ion exchange capacity, etc.) affects their morphology, water uptake, and proton conductivity under various environmental conditions (temperature and relative humidity). The synthesis of these relatively well-defined graft structures involves three reaction steps, including the preparation of PVDF copolymers containing a few mol% of chlorotrifluoroethylene (CTFE) units, the ATRP graft-from reaction to incorporate several polystyrene side chains, and the subsequent sulfonation reaction on the PS side chains. The PVDF-g-SPS graft copolymer with a combination of a high PVDF backbone molecular weight (M_n >300 000 g/mol), very low SPS graft density (0.3 mol%), and high graft length (SPS content >30 mol%) presents an interesting material for the proton exchange membrane (PEM). This graft copolymer self-assembles into a microphase-separated morphology with randomly oriented long-range lamella/cylinder ionic channels (with small widths) that are imbedded in the hydrophobic semicrystalline PVDF matrix. This graft copolymer morphology offers a high ion exchange capacity (IEC = 2.75 mmol/g) and resistance to excessive water swelling, which yields notably higher proton conductivity than Nafion under 30−120 °C and high humidity conditions.

Introduction

The proton exchange membrane fuel cell (PEMFC), a promising power resource without green house gas emission, has promoted considerable research interests in chemistry, physics, and theory.[1−5] The proton exchange membrane (PEM) is a key component in PEMFC, which serves as both an electrolyte and separator. Due to the demanding environment and functions, an ideal PEM material[1−3] requires a combination of chemical and physical properties: long-term chemical and electrochemical stability in the reducing environment at the cathode and the harsh oxidative environment at the anode, good mechanical strength and dimension stability in tight PEM stacks, and high proton conductivity under various operation conditions (i.e., temperatures and relative humidity). Numerous polymers have been designed and studied in the past decades with some successes and limitations. These polymers are mainly classified as fluoropolymers[6−8] and aromatic hydrocarbon polymers.[9−11] The most commonly known is Nafion (sulfonated fluoropolymer), which shows good stability and good proton conductivity in low temperature and high relative humidity conditions. However, this Nafion-based PEM is expensive, and its conductivity dramatically decreases at elevated temperatures (>80 °C) and low humidity (<40%) conditions. On the other hand, the membrane based on phosphoric acid-doped polybenzimidazole[12,13] can reach reasonably high proton conductivity at 120−200 °C, without any water management. The higher temperature allows for better efficiency and power densities and reduces the sensitivity to carbon monoxide poisoning. However, these type of membranes exhibit low proton conductivity, especially in low temperature environments.

Sulfonated polystyrene (SPS)[14]-based PEM was investigated in the 1960s and showed high water swelling and inadequate chemical stability due to the tertiary C−H bonds. In order to improve its properties, the sulfonated polystyrene was grafted onto fluoropolymers, including poly(tetrafluoroethylene-co-hexafluoropropylene)[15] and poly(vinylidene fluoride)[16−18] polymer backbones. This chemistry involves an irradiation-mediated free radical polymerization process using monomer-bearing sulfonic acid or styrene followed by a sulfonation reaction of benzyl groups. The lifetime of fuel cells based on this graft copolymer system has been extended to 5000 h at 85 °C,[19] with the benefits of reduced water uptake and high proton conductivity. Unfortunately, the polymer structure and morphology were poorly controlled and rarely characterized, since the irradiation initiating process results in very complicated molecular structures. More recently, some efforts have been devoted to synthesizing well-defined fluoropolymer/polystyrene block copolymers,[20,21] with a subsequent sulfonation reaction to form the corresponding sulfonated polymer structures[22,23] that exhibit a microphase separation between hydrophobic and hydrophilic domains. The experimental results show that the conductivity and water swelling of the membrane are strongly related to the chemical structure and morphology and are proportional to the ion-exchange capacity (IEC). However, their proton conductivities are generally smaller than that of Nafion (a random copolymer) under the same IEC value. Interestingly, one paper[24] directly compares fluoropolymer/sulfonated polystyrene diblock

* Corresponding author: chung@ems.psu.edu.
† Department of Materials Science and Engineering.
‡ The Energy Institute.
§ Department of Energy and Geo-Environmental Engineering.
∥ Department of Crop and Soil Sciences.
⊥ Current address: Department of Applied Chemistry, School of Sciences, Xi'an Jiaotong University, Shaanxi, 710049, China.

10.1021/ma801277m CCC: $40.75
Published on Web 11/11/2008

and graft copolymers containing ~25 mol% SPS content, although these two polymers have a very different molecular weight range (more than 1 order of magnitude). The graft copolymer, having high graft density and low graft length, bears "cluster-network" ionic domains, similar to that of Nafion, which yields membranes with better mechanical properties and resistance to water swelling and dissolution. Some graft copolymers[24] with high IEC >2 mmol/g show similar proton conductivity as that of Nafion 117 (IEC = 0.9 mmo/g). In contrast, the diblock copolymer membrane, possessing a well segregated and oriented lamellar morphology with long-range ionic order, shows significantly higher proton conductivity (in-plane) than the graft copolymer with the same IEC. However, the combination of in-plane lamella morphology and low molecular weight of the diblock copolymer also leads to excessive swelling and instability in the membrane. More importantly, it lowers the proton conductivity in the through-plane direction that is most relevant to proton conduction in fuel cells.

The ideal PEM should simultaneously provide high through-plane proton conductivity and good dimensional stability to resist excess water swelling or shrinking under various environmental conditions (i.e., temperatures and humidities). The attainment of a desirable polymer structure and morphology remain as interesting scientific challenges. Intuitively, a dimensionally stable PEM structure may involve a 3-D hydrophobic (preferred crystalline) matrix with good mechanical properties, in which many hydrophilic microsize ionic channels (cylinders or lamellas with preferred through-plane orientation) across the membrane matrix are all meant to provide proton conductivity. The combination of strong acidity, high acid concentration, and good proton mobility is essential for high conductivity and suitable water content, offering good proton mobility without diluting the proton concentration. In addition, the hydrophilic polymer chains should anchor to the solid hydrophobic matrix; a high concentration of ions (high IEC) with the associated water molecules can be stationed in the hydrophilic domains without the concern for water dissolution. It is curious to understand such a hydrophobic−hydrophilic separated morphology responding to elevated temperature and low humidity conditions.

It is worthwhile to systematically investigate poly(vinylidene fluoride)-*g*-sulfonated polystyrene (PVDF-g-SPS) graft copolymer system. A complete range of relatively well-defined graft copolymers with various compositions and microstructures can be prepared, which provides a fair side-by-side comparison of how polymer microstructures (on characteristics of backbone molecular weight, graft density, graft length, IEC, etc.) affect the morphology (sphere, cylinder, bicontineous, lamella, etc.),[25,26] water uptake, and proton conductivity under various conditions. In addition, the graft copolymer, having a nonlinear molecular structure, can form isotropy SPS ionic channels (without specific orientation), imbedded in the hydrophobic (highly crystalline) PVDF matrix, which provide similar in-plane and through-plane conductivity.[24]

Experimental Section

Materials. Triethylboron (TEB) and other chemicals were purchased from Aldrich and used as received unless otherwise noted. Tetrahydrofuran (THF) was dried and distilled from sodium benzophenone ketyl under nitrogen. Vinylidene fluoride (VDF) and CTFE monomers, purchased from SynQuest Laboratory Inc., were quantified in a freeze−thaw process prior to use. Styrene was passed through a column of neutral alumina to remove inhibitors; it was then distilled before use. Low molecular weight P(VDF-co-CTFE)s (M_n = 15 000−20 000 g/mol) were synthesized by a procedure described in our previous reports.[27,28] A commercial P(VDF-co-CTFE) (CTFE content = 6 mol%) copolymer (PVDF SOLEF 31008/1001) with a high molecular weight (M_n = 312 000 g/mol) was kindly provided by Solvay. To reduce the CTFE content, which determines the branch density in the PVDF-g-PS graft copolymer, a hydrogenation process[29] was employed to convert some CTFE units to TrFE (trifluoethylene) units to obtain P(VDF-ter-TrFE-ter-CTFE) terpolymers that have a CTFE content from 1 to 6 mol%. Since VDF and TrFE units are cocrystallizable, a small amount of TrFE units do not have any significant effect to the polymer morphology and melting temperature.

Synthesis of PVDF-g-PS Copolymers. The synthesis of PVDF-g-PS graft copolymers began with P(VDF-co-CTFE) copolymers and P(VDF-ter-TrFE-ter-CTFE) terpolymers, containing C−Cl moieties (CTFE units) that involve atom transfer radical polymerization (ATRP) with styrene monomers.[21] In a typical graft reaction, 2.0 g of the P(VDF-co-CTFE) copolymer together with 125 mg of CuCl (1.3 mmol) was dissolved in 40 mL of NMP in a 100 mL three-neck flask with a magnetic stir bar under an inert atmosphere. A controlled amount of styrene was then injected into the P(VDF-co-CTFE) solution. Separately, 500 mg of 2,2-bipyridine (BPy, 3.2 mmol) was dissolved in 10 mL of NMP in a 25 mL Schlenk flask under an inert atmosphere, which was transferred into the reaction flask by a N_2-purged syringe. The reaction flask was then immersed in an oil bath at 120 °C. After 24 h, the polymerization was terminated by cooling to room temperature and exposing to air. The reaction mixture was diluted with acetone and then passed through a column filled with silica gel, followed by precipitation in methanol. The resulting PVDF-g-PS graft polymer was dried in a vacuum oven at 60 °C overnight.

Sulfonation Reaction of PVDF-g-PS Copolymers. The sulfonation reaction was carried out in 1,2-dichloroethane solvent, following previously reported procedures.[30] Typically, in a 100 mL three-neck flask that was nitrogen-purged, equipped with a dropping funnel, and condenser, 40 mL of 1,2-dichloroethane and 2.0 g of PVDF-g-PS were added, and the mixture was heated to 50 °C under stirring until the copolymer completely dissolved. Acetyl sulfate was prepared by injecting 3 mL of acetic anhydride and 10 mL of dichloroethane into a nitrogen-purged vial. The solution was cooled to 0 °C in an ice bath, and 1 mL of 95−97% sulfuric acid was injected. The resulting acetyl sulfate solution was immediately transferred to the polymer solution at 40 °C using a dropping funnel. Samples were periodically extracted and precipitated in 50/50 ethanol/hexane mixture for determining their sulfonation levels. The precipitate was washed with water until the residual water had a pH = 7. The sulfonated polymers were dried under vacuum at ambient temperature overnight. For some graft copolymers, multiple sulfonation reactions were performed to achieve higher sulfonation levels.

Polymer Structure Characterization and Instrumentations. ^{1}H and ^{19}F NMR spectra were recorded on a BrukerAM-300 spectrometer, which provide the composition information of the copolymers, including the degree of sulfonation (DS). The thermal transition data was obtained in a TA Instruments Q100 differential scanning calorimeter (DSC) at a heating rate of 10 °C/min. The thermogravimetric analysis (TGA) was performed in a TA Instruments model 2950 at a heating rate of 20 °C/min, from room temperature to 700 °C. The molecular weight was determined using a Waters 150C operated at 70 °C. The columns used were mStyragelHT of 10^6, 10^5, 10^4, and 10^3, with a flow rate of 0.7 mL/min and the mobile phase of *N*,*N*-dimethylformamide (DMF). Narrow molecular weight distribution PMMA samples were used as standards for determining the polymer molecular weight.

Membrane Preparation and Evaluation. Membranes were prepared by dissolving the sulfonated graft copolymers in THF and followed by casting onto a Teflon substrate. Films were dried at room temperature for several hours before heating at 60 °C for 2 h under vacuum. The sulfonated membranes were treated with 2 M HCl overnight. They were then washed several times with deionized water for 30 min periods. Membrane morphology was observed by transmission electron microscopy (TEM) using JEOL JEM-1200 equipment. The PEM films were microtomed to yield slices with a thickness ~100 nm, which were stained with ruthenium tetraoxide before embedding in expoxy resin for TEM measurement. To determine the water uptake and water content λ (molar ratio of

Scheme 1

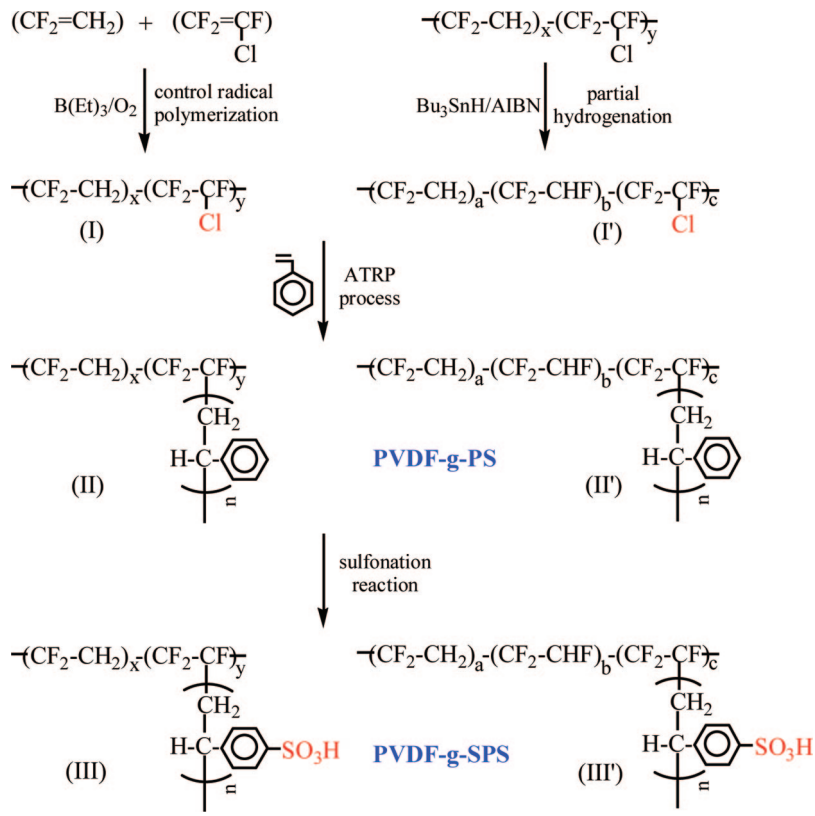

water to sulfonic acid) vs IEC, the membrane was dried under vacuum for 12 h at 70 °C and cooled to room temperature in a desiccator before measuring the weight in "dry" state (W_d). The membrane was then equilibrated in deionized water overnight at room temperature. After removal of the water from the surface, the weight in "wet" state (W_w) was measured. The water uptake of the membrane was calculated to determine the percent weight increase from "dry" to "wet" states, $[(W_w - W_d)/W_d] \times 100\%$. With the known water uptake and sulfonic acid content (NMR results), the water content λ was then calculated. In addition, the ion exchange capacity (IEC) was calculated in millimoles of sulfonic acid in 1 g of the polymer. It has been reported[23] that the calculated IEC number coincides very well with the one based on titration.

The membrane conductivity was tested using a BekkTech conductivity cell (BT 115), which was assembled in an ElectroChem fuel cell hardware. The relative humidity (RH) in the cell was achieved by feeding it with humidified nitrogen gas, by passing the gas flow through a humidification column. To yield the desired water vapor activity in the cell, temperatures of the cell and humidification column were controlled. The RH value in the cell was calculated from the ratio of the saturated water vapor pressures, respectively, at the temperatures of the humidification column $P(T_h)$ and the cell $P(T_c)$: RH (%) = $P(T_h)/P(T_c) \times 100$. The BekkTech Test Protocol was applied for conductivity tests, including the sample preparation and testing procedure. The sample was cut to approximately 5 mm × 20 mm. Testing was performed at 25 °C and 120 kPa and at 120 °C and 230 kPa (cell pressure). An input flow rate was in a range of 290−390 cm^3/min. A sample was conditioned at 70% RH for 2 h before the conductivity measurement. In the subsequent change of RH, a stabilization time about 1 h was implemented before each measurement. The membrane resistance measurements were performed by a four-probe method with a Gamry electrochemical impedance spectroscopy system. For some (highly conductive) membranes, data was collected using AC or DC methods. Both methods produced the same result, indicating a pure resistor. When DC voltage sweeps from 0.1 to −0.1 V were performed, the voltage was linear with respect to current. For the AC sweep, the measured impedance was independent of frequency, and the phase angle was essentially zero in different frequency ranges for different membranes. Conductivity (in-plane) was calculated using the sample thickness (T), sample width (W), distance between the sensor electrodes in the conductivity cell (L), and the membrane resistance (R) from the equation $\sigma = L/W \times T \times R$.

Results and Discussion

In this paper, we have developed a research strategy to prepare two families of PVDF-g-SPS graft copolymers based on a low and a high molecular weight of PVDF backbones, followed by a variation of branch density, branch length, and sulfonation levels. The graft copolymers were then systematically evaluated by comparing their molecular microstructures, morphologies, water uptakes, and proton conductivities under various environmental conditions (temperature and relative humidity).

Synthesis and Structure Characterization. Two families of low molecular weight P(VDF-co-CTFE) copolymers (I) and high molecular weight P(VDF-ter-TrFE-ter-CTFE) terpolymers (I′) were employed as the starting polymers in the preparation of PVDF-g-SPS graft copolymers, as illustrated in Scheme 1. The low molecular family of P(VDF-co-CTFE) copolymers, having M_n = 15 000−20 000 g/mol and a CTFE content from 1.0 to 4.6 mol% were prepared by a copolymerization reaction, mediated by TEB/O_2 initiator (TEB: triethylborane).[27,28] On the other hand, the high molecular set of P(VDF-ter-TrFE-ter-CTFE) terpolymers, having few % of TrFE units, and a CTFE content from 1 to 6 mol%, were prepared by a partial hydrogenation[29] of a commercial P(VDF-co-CTFE) copolymer, with 6 mol% of CTFE units and M_n = 312 000 g/mol. The hydrogenation reaction is very efficient and selective with interconverting some CTFE units to TrFE units, without changing polymer molecular weight.

Both P(VDF-co-CTFE) copolymers (I) and P(VDF-ter-TrFE-ter-CTFE) terpolymers (I′) were then applied in the subsequent ATRP graft-from polymerization of styrene, followed by the

Table 1. A Summary of PVDF-g-PS (II) and PVDF-g-SPS (III) Graft Copolymers Prepared from Several Low Molecular Weight (VDF-co-CTFE) Copolymers (I)

P(VDF-co-CTFE) (I)			PVDF-g-PS (II)[a]			PVDF-g-SPS (III)[d]		
run	VDF/CTFE (mole ratio)	St (g)	VDF/St (mole ratio)	graft[b] density	graft[c] length	VDF/St/SSt[e] (mole ratio)	DS (%)	IEC (mmol/g)
A1-1	99.0/1.0	1	99.0/5.3	0.4	13.2	99.0/2.2/3.1	58.0	0.43
A1-2	99.0/1.0	3	99.0/17.7	0.4	44.3	99.0/4.2/13.5	76.1	1.44
A1-3	99.0/1.0	3	99.0/17.7	0.4	44.3	99.0/2.1/15.6	88.0	1.64
A1-4	99.0/1.0	6	99.0/31.5	0.4	78.8	99.0/11.3/20.2	64.2	1.78
A1-5	99.0/1.0	6	99.0/31.5	0.4	78.8	99.0/10.3/21.2	67.4	1.86
A1-6	99.0/1.0	6	99.0/31.5	0.4	78.8	99.0/0.0/31.5	100	2.57
A2-1	98.0/2.0	1.5	98.0/13.8	0.8	17.3	98.0/5.1/9.9	71.9	1.12
A2-2	98.0/2.0	1.5	98.0/13.8	0.8	17.3	98.0/2.5/12.5	83.0	1.38
A2-3	98.0/2.0	3	98.0/21.5	0.8	26.9	98.0/3.7/18.1	83.0	1.77
A2-4	98.0/2.0	3	98.0/21.5	0.8	26.9	98.0/2.2/19.3	89.6	1.88
A2-5	98.0/2.0	3	98.0/21.5	0.8	26.9	98.0/1.6/19.9	92.7	1.93
A2-6	98.0/2.0	5	98.0/54.2	0.8	67.8	98.0/12.5/41.7	76.9	2.70
A3-1	96.6/3.4	1.8	96.6/14.1	1.4	10.1	96.6/6.5/7.6	46.1	0.88
A3-2	96.6/3.4	1.8	96.6/14.1	1.4	10.1	96.6/2.8/11.3	80.2	1.26
A3-3	96.6/3.4	2.4	96.6/23.6	1.4	16.9	96.6/7.6/16.0	67.7	1.55
A3-4	96.6/3.4	2.4	96.6/23.6	1.4	16.9	96.6/4.9/18.7	79.2	1.78
A3-5	96.6/3.4	3	96.6/36.4	1.4	26.0	96.6/8.9/27.5	75.7	2.19
A3-6	96.6/3.4	3	96.6/36.4	1.4	26.0	96.6/6.8/29.6	81.2	2.32
A4-1	95.4/4.6	1.8	95.4/15.1	1.8	8.4	95.4/7.4/7.7	50.8	0.87
A4-2	95.4/4.6	1.8	95.4/15.1	1.8	8.4	95.4/5.0/10.1	67.1	1.12
A4-3	95.4/4.6	2.3	95.4/22.5	1.8	12.5	95.4/7.4/15.1	67.1	1.48
A4-4	95.4/4.6	2.3	95.4/22.5	1.8	12.5	95.4/1.4/21.1	93.6	1.98
A4-5	95.4/4.6	2.5	95.4/25.5	1.8	14.2	95.4/0.6/24.9	97.5	2.21

[a] ATRP graft reaction condition: a mixing solution of 2 g of P(VDF-co-CTFE), 0.125 g of CuCl, 0.5 g of BPy, 40 mL of NMP and a specific amount of styrene was stirred at 120 °C for 24 h. [b] Number of PS grafts per 100 VDF units in the backbone, estimated from 40% of CTFE units in the copolymer (I) involving ATRP graft-from reaction. [c] Number of styrene units in each graft, calculated from the styrene mole ratio divided by graft density. [d] Sulfonation reaction condition: a mixing solution of 1 g of PVDF-g-PS (II), 1 mL of H_2SO_4, 3 mL of acetic anhydride, and 40 mL of 1,2-dichloroethane was performed at 50 °C. [e] St: styrene; SSt: sulfonated styrene.

Table 2. A Summary of PVDF-g-PS (II′) and PVDF-g-SPS (III′) Graft Copolymers Prepared from Several High Molecular Weight Poly(Vdf-ter-TrFE-ter-CTFE) Terpolymers (I′)

P(VDF-terTrFE-ter-CTFE) (I′)			PVDF-g-PS (II′)			PVDF-g-SPS (III′)		
run	VDF/TrFE/CTFE (mole ratio)	St (g)	VDF/St (mole ratio)	graft[a] density	graft[b] length	VDF/St/SSt[c] (mole ratio)	DS (%)	IEC (mmol/g)
B1-1	94.0/5.2/0.8	4.6	94.0/36.1	0.3	120	94.0/17.2/18.9	55.1	1.60
B1-2	94.0/5.2/0.8	4.6	94.0/36.1	0.3	120	94.0/0.0/36.1	100	2.75
B2-1	94.0/3.9/2.1	3.0	94.0/29.4	0.8	37	94.0/11.1/8.3	62.1	1.65
B2-2	94.0/3.9/2.1	3.0	94.0/29.4	0.8	37	94.0/4.0/25.4	86.3	2.18
B3-1	94.0/2.6/3.4	3.0	94.0/29.5	1.4	21	94.0/18.0/11.5	39.0	1.08
B3-2	94.0/2.6/3.4	3.0	94.0/29.5	1.4	21	94.0/3.3/26.2	88.9	2.23
B4-1	94.0/1.7/4.3	3.1	94.0/28.1	1.7	17	94.0/14.2/13.9	50.4	1.32
B4-2	94.0/1.7/4.3	3.1	94.0/28.1	1.7	17	94.0/1.5/26.6	94.7	2.28
B5-1	94.0/0.0/6.0	4.0	94.0/32.7	2.4	14	94.0/14.7/18.0	54.9	1.56
B5-2	94.0/0.0/6.0	4.0	94.0/32.7	2.4	14	94.0/6.0/26.7	81.7	2.18

[a] Number of PS grafts per 100 VDF units in the backbone, estimated from 40% of CTFE units in the copolymer (I′) involving ATRP graft-from reaction. [b] Number of styrene units in each graft, calculated from the styrene mole ratio divided by graft density. [c] St: styrene; SSt: sulfonated styrene.

sulfonation reaction of PS grafts. As shown in Scheme 1, the reactions produce the intermediate P(VDF-co-CTFE)-g-PS (II) and P(VDF-ter-TrFE-ter-CTFE)-g-PS (II′), and the final P(VDF-co-CTFE)-g-SPS (III) and P(VDF-ter-TrFE-ter-CTFE)-g-SPS (III′) graft copolymers, respectively. Since both P(VDF-co-CTFE) and P(VDF-ter-TrFE-ter-CTFE) backbones in all graft copolymers contain ~95% VDF units, and both VDF and TrFE units are cocrystalizable, they are basically PVDF polymers with properties that are controlled by backbone molecular weight, graft density, and graft length. For simplicity's sake, they are identified as PVDF-g-PS (II and II′) and PVDF-g-SPS (III and III′) graft copolymers, respectively.

The detailed polymer structure characterizations are discussed in the Supporting Information. Tables 1 and 2 summarize the experimental results of two graft copolymer systems from low molecular weight P(VDF-co-CTFE) copolymers (I) and high molecular weight P(VDF-ter-TrFE-ter-CTFE) terpolymers (I′), respectively. For studying polymer microstructure effects, the graft copolymers were systematically varied with graft density, graft length, degree of sulfonation (DS), and ion exchange capacity (IEC). In each system, we started with several copolymers (I) or terpolymers (I′) containing 1−6 mol% of CTFE units, which provided the graft points in the corresponding graft copolymers. During the ATRP graft reaction, various amounts of styrene (St) were added to control the graft length in the PVDF-g-PS graft copolymer. The graft length (average styrene repeating units per PS graft) in the PVDF-g-PS copolymer was calculated from the styrene incorporation (^{1}H NMR) and graft density (40% of the CTFE units in the starting polymer; estimated by ^{19}F NMR). The same graft density and graft length are expected in the corresponding PVDF-g-SPS graft copolymer. On the other hand, the DS value is determined from the ^{1}H NMR spectrum of the PVDF-g-SPS copolymer, by estimating the relative peak intensity between aromatic protons in styrene (St) units and sulfonated styrene (SSt) units. It is interesting to note that DS of the PVDF-g-PS copolymer is quite dependent on its PS content and graft density. The copolymer with a lower PS content or higher grafting densities requires a longer sulfonation period or rigorous sulfonation condition. To achieve a high DS in these samples, multiple sulfonation reaction

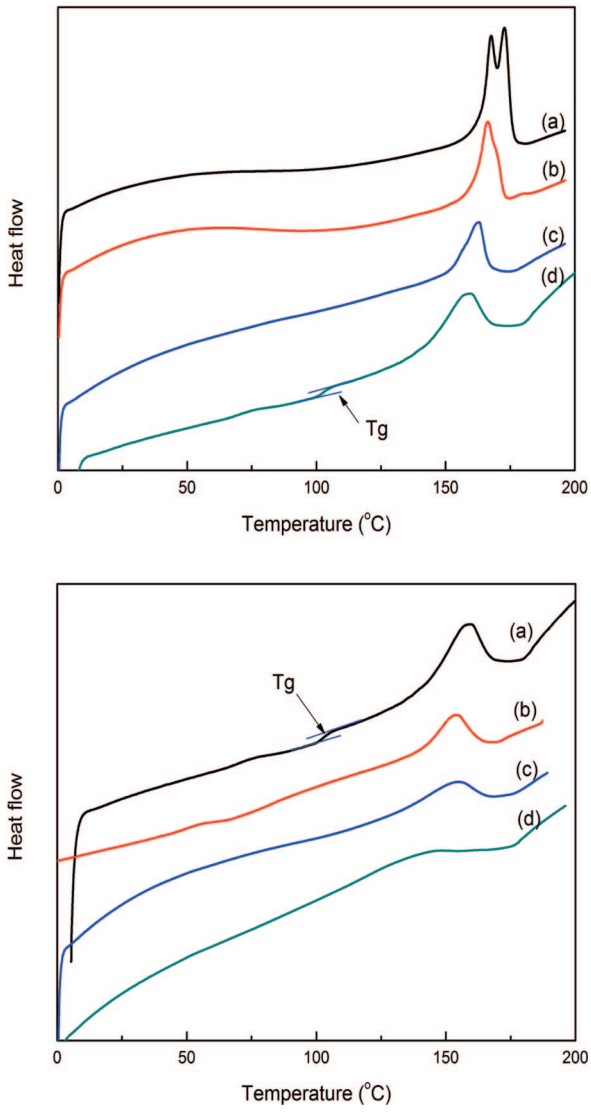

Figure 1. (top) Comparison of DSC curves between (a) a starting P(VDF-co-CTFE) copolymer (I) and three corresponding PVDF-g-PS graft copolymers (II) with 0.4 mol% graft density and various PS graft length (b) 13.2, (c) 44.3, and (d) 78.8 average styrene units per graft, respectively; (bottom) DSC curve of four PVDF-g-PS graft copolymers having similar PS graft content (VDF/St ~ 100/30 mol ratio) but different graft density (a) 0.4, (b) 0.8, (c) 1.4, and (d) 1.8 mol%, respectively.

processes have been applied. The ion exchange capacity (IEC) is then calculated from the DS value by estimating the sulfonic acid concentration in the final PVDF-g-SPS graft copolymer. Overall, we have applied three well-controlled reactions: co-polymerization (or hydrogenation), ATRP graft reaction, and sulfonation, in order to prepare a wide range of PVDF-SPS graft copolymers with various molecular weight, graft density, graft length, and sulfonic acid concentration. This offers us the opportunity to systematically examine the effects of the polymer microstructure on proton conductivity and water uptake under various conditions (temperature and relative humidity).

Thermal Properties and Morphologies. Since the graft copolymers contain a crystalline backbone and amorphous side chains, it is convenient to apply DSC and TEM techniques to understand their morphologies and thermal properties. Figure 1 (top) compares DSC curves of three PVDF-g-PS graft copolymers (II) (Set A1 in Table 1), which have the same (0.4 mol%) graft density and various PS graft length (13.2, 44.3, and 78.8 average styrene units per graft, respectively). The starting copolymer (I) shows a melting temperature (T_m) at 162.5 °C. The increase of PS content leads to only a less than 4 °C decrease in T_m, and the decrease of heat of fusion (ΔH) is mainly due to the dilution effect. As the molecular weight of the PS graft increases, the T_g of the PS domain appears at 100 °C. The coexistence of the T_m for the P(VDF-co-CTFE) backbone and the T_g for the PS grafts indicates a clear microphase separation morphology in this PVDF-g-PS (99/31.5 mol ratio) graft copolymer. Overall, with low graft density the PS graft length, residing in the amorphous phase, has only a small effect to the PVDF crystalline phase. On the other hand, Figure 1 (bottom) compares four PVDF-g-PS graft copolymers having similar PS graft contents (VDF/St ~ 100/30 mol ratio) but different graft densities (0.4, 0.8, 1.4, and 1.8 mol%, respectively). With the increase of graft density, the crystallinity and heat of fusion (ΔH) decreased, and the T_g of the PS graft becomes undetectable due to low molecular weight. The PVDF-g-PS graft copolymer, having 1.8 mol% graft density, shows almost no melting point and no T_g, implying a poor phase separation. Overall, the morphology of the PVDF-g-PS graft copolymer is largely controlled by graft density.

It is interesting to examine the effects of sulfonation to the thermal property and morphology of the PVDF-g-PS graft copolymer, which alters the hydrophobic PS grafts to the hydrophilic SPS grafts, along with the ability to absorb a significant amount of water molecules. Since the sulfonation of PS is statistically random, the partially sulfonated PS grafts are essentially random copolymers. Figure 2 (top) compares DSC curves of a PVDF-g-PS (II) graft copolymer, having a VDF/St = 99.0/31.5 mol ratio and graft density = 0.4 mol%, and two corresponding sulfonated PVDF-g-SPS (III) graft copolymers, with 64.2% (run A1−4) and 100% (run A1−6) degrees of sulfonation (DS). After sulfonation, the graft copolymers show similar T_m, but lower ΔH. The value of ΔH is gradually decreased as more benzyl sulfonic acids are introduced to the PS grafts, which is largely due to the dilution effect. Figure 2 (bottom) compares four PVDF-g-SPS graft copolymers, which were prepared by complete sulfonation of the corresponding PVDF-g-PS graft copolymers. In other words, all PVDF-g-SPS graft copolymers (III) have similar SPS contents (VDF/SSt ~ 100/30 mol ratio) and different graft densities (0.4, 0.8, 1.4, and 1.8 mol%, respectively). The side-by-side comparison, before and after sulfonation, also shows a small effect to the T_m of the PVDF backbone in all compositions, but it also shows a reduction of the overall crystallinity, which may be mostly associated with the bulkiness of benzyl sulfonic acid with the absorbed water molecules.

Figure 3 shows TEM micrographs of the cross-sectional slices of three representative PVDF-g-SPS graft copolymers (runs A1−6, A3−6, and B1-2). In general, they are not as well ordered as the typical morphologies in diblock copolymers. Comparing the first two graft copolymers (III), they have the same low molecular weight PVDF backbone, similar SPS contents (VDF/SSt ~ 100/30 mol ratio), and different graft densities (0.4 and 1.4 mol%, respectively) and graft lengths (79 and 26 SSt units, respectively). The membrane morphology is clearly affected by graft density and graft length. As predicted by theory,[25,26] the morphology of the graft copolymer is controlled by a combination of volume fraction, graft density, and graft length. The A3−6 sample with higher graft density and lower graft length (Figure 3a) shows a cluster-network morphology with a cluster diameter ~5 nm, similar to that of Nafion. On the other hand, Figure 3b shows many long-range ionic channels (10−15 nm in width) with no specific spatial ordering in the A1−6 sample that possesses low graft density and high graft length. The morphology seems to contain largely lamella structures, and it may also include some cylinder

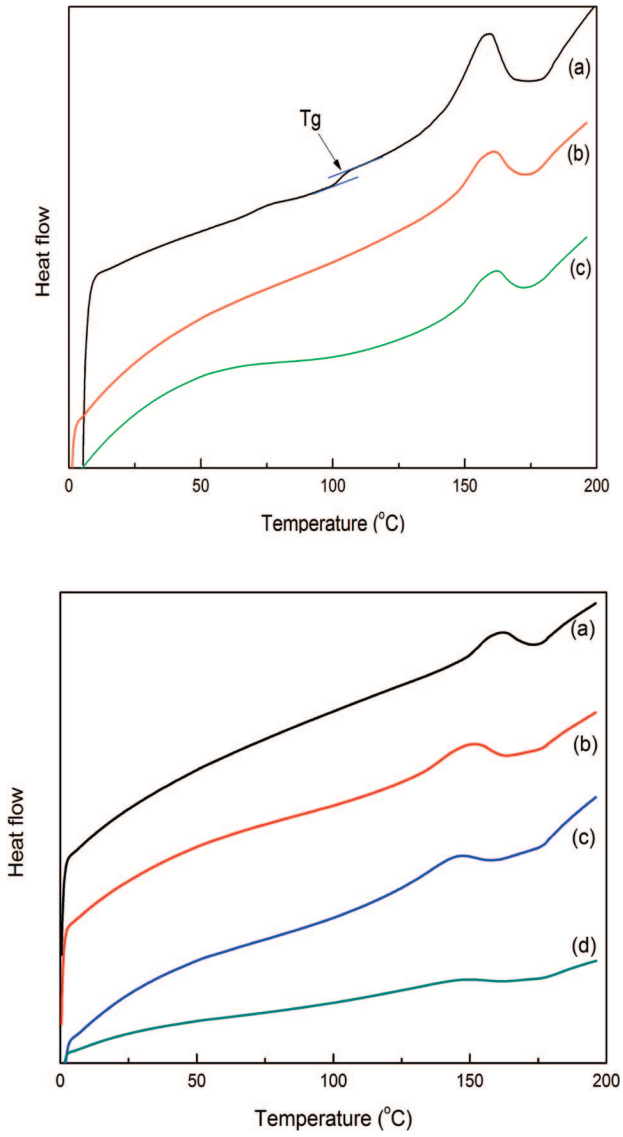

Figure 2. (top) DSC curves of (a) PVDF-g-PS (II) graft copolymer having VDF/St = 99.0/31.5 mol ratio and two corresponding sulfonated PVDF-g-SPS (III) graft copolymers with (b) 64.2 and (c) 100% degree of sulfonation (DS); (bottom) DSC curve of four PVDF-g-SPS graft copolymers having similar SPS graft content (VDF/SSt ~ 100/30 mol ratio) but different graft density (a) 0.4, (b) 0.8, (c) 1.4, and (d)1.8 mol%, respectively.

structures. Overall, it is not as well-ordered a morphology as those in the block copolymers. Figure 3c shows a TEM micrograph of the B1-2 sample that has more than 10 times the amount of PVDF molecular weight than the A1−6 sample, with higher SPS graft length (120 SSt units; VDF/SSt 94/36.1 mol ratio) and lower graft density (0.3 mol%). Better ordered lamella/cylinder morphology with a smaller channel width of 5−10 nm was observed in the B1-2 membrane. The smaller channel width also showed lower water uptake and resistance to water swelling (discussed later).

Water Uptake. Water uptake is a key characteristic in PEM, which is determined by the percentage of weight increase due to the absorbed water molecules in the membrane. Figures 4 and 5 show water uptake (wt%) and water content λ (molar ratio of water to sulfonic acid) vs IEC at room temperature for all PVDF-g-SPS graft polymers in Tables 1 and 2, respectively. They include both low and high molecular weight PVDF backbone systems with various graft densities and IEC values. The plotted lines are used solely for guiding purposes when viewing. It is generally known that the water uptake and water content (λ) are directly relative to the sulfonic acid concentration and IEC value, and both sharply increase over a critical IEC value that is associated with the threshold of forming the cohesive ionic (hydrophilic) domains. In these graft copolymers, all factors, including water uptake, water content, critical IEC value, and water-dissolution point, are dependent on the graft copolymer microstructure, a combination of backbone molecular weight, graft density, and graft length.

For the low molecular weight PVDF-g-SPS (III) graft copolymers with the same IEC value (Figure 4), both water uptake and water content (λ) are inversely proportional to graft density. Lower graft density in sets A1 and A2 results in higher water uptakes and λ values. In detail, the critical IEC value changes from 1.5 mmol/g in the A1 set with a graft density of 0.4 mol%, to 2.0 mmol/g in the A4 set with a graft density of 1.8 mol%. Over the critical IEC values, the A1 and A2 graft copolymers also exhibit a sharper increase in water uptakes and λ values. The λ values reach >80 in sets A1 and A2, which are between the λ values reported in diblock and graft copolymers.[24] On the other hand, the maximum λ values (~40) in sets A3 and A4 are close to the reported value in the graft copolymer that also has high graft density. It is clear that the PVDF-g-SPS graft copolymer (III) with low graft density is more sensitive to water uptake, especially in the low IEC region. The longer consecutive PVDF and SPS segments form longer range continuous lamella/cylinder ionic channels, as shown in Figure 3b, increase the water sensitivity and overall water uptake. On the other hand, the graft copolymers with higher graft density and lower graft length, having more dispersed cluster morphology with many small ionic domains imbedded in the hydrophobic PVDF matrix (Figure 3a), shows more resistant in absorbing water molecules. With a further increase of the IEC value, the PVDF-g-SPS graft copolymer becomes water soluble. It is interesting to note that despite the lower water sensitivity in A3 and A4 graft copolymers, they become water soluble at a lower IEC value >2.25. The A1 and A2 graft copolymers show a higher water dissolution point at an IEC value >2.6. The crystallinity of the hydrophobic PVDF matrixes in the A1 and A2 sets (curves a and b in Figure 2(bottom)) are higher than those in the A3 and A4 sets (curves c and d in Figure 2(bottom)), which may offer the needed stability of PEM to resist water dissolution in the high IEC range.

Surprisingly, the PVDF backbone molecular weight has a significant effect to the water swelling behavior in the graft copolymer (III′), as shown in Figure 5. The water uptake, λ value, and critical IEC value become less sensitive to the graft density in the high molecular weight graft copolymers. Four PVDF-g-SPS samples (III′), having similar IEC values ~2.20 mmol/g but very different graft densities (0.8, 1.4, 1.7, and 2.4 mol%), exhibit similar water uptakes between 170% and 227% and λ values of 48, 42, 55, and 54, respectively. The backbone molecular weight effect is particularly important for the graft copolymers with very low graft density and high IEC value. Comparing A1−6 and B1-2 PEMs, both have similar low graft densities (0.4 vs 0.3 mol%) and IEC values (2.57 vs 2.75mmol/g), the higher molecular weight B1-2 graft copolymers (III′) consistently shows only about half of the water uptake than that of the corresponding lower molecular weight A1−6 graft copolymers (III). The TEM micrographs in Figure 3b,c confirm the difference with a significantly larger hydrophilic ion channel width in the A1−6 sample than in the B1-2 sample. Although the B1-2 graft copolymer has a very high IEC value of 2.75 mmol/g, it only shows a relatively mild water uptake of 254% with a λ value of 53. More importantly, it maintains good film integrity. In contrast, the corresponding A1 sample with IEC

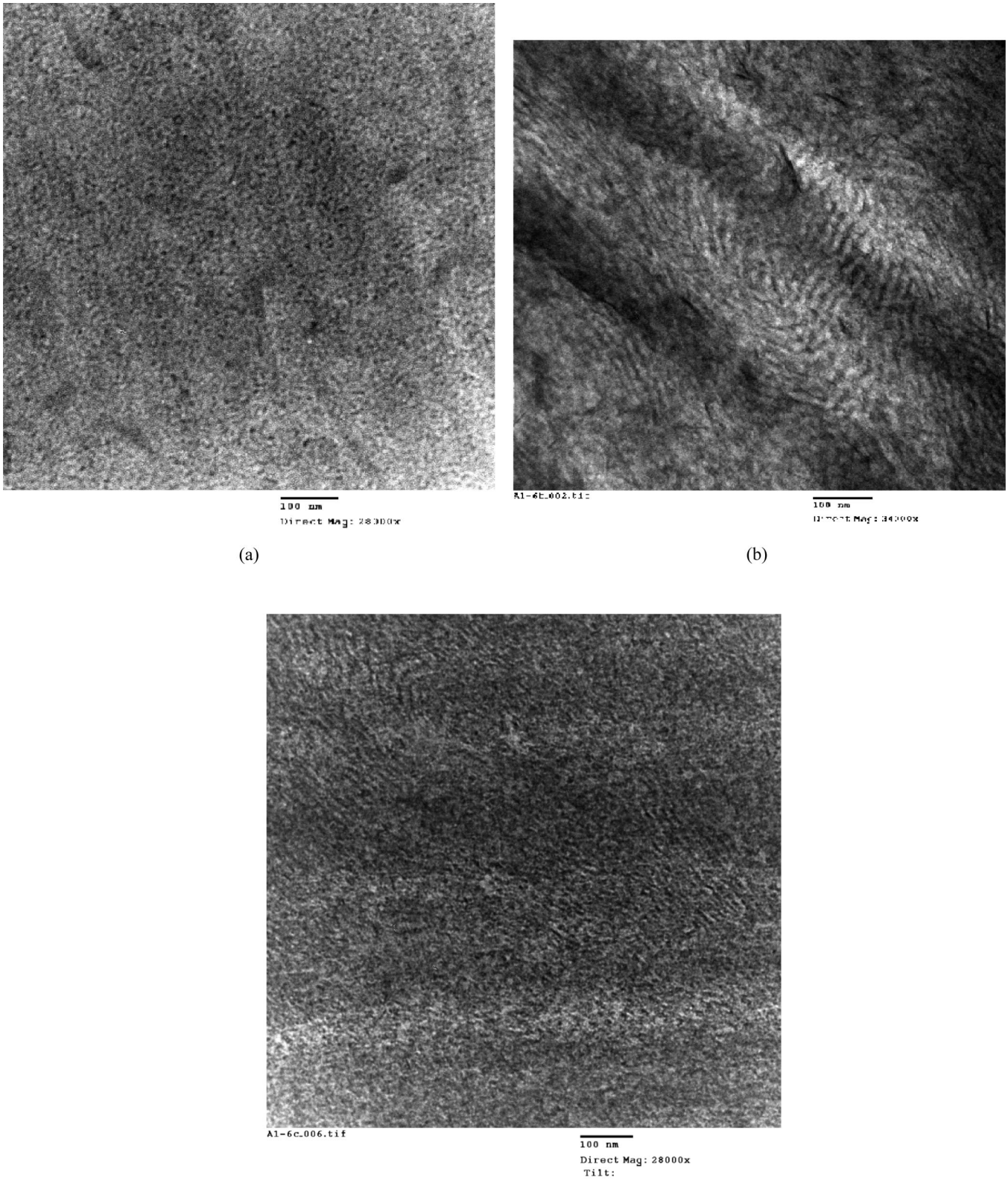

Figure 3. TEM micrographs of three PVDF-g-SPS graft copolymers including (a) run A3−6, (b) run A1−6, and (c) run B1-2.

> 2.57 is completely water soluble. As will be discussed later, this B1-2 sample exhibits proton conductivity higher than that for Nafion under high humidity conditions. The combination of a high PVDF molecular weight and low graft density in the graft copolymer (III′) results in high crystallinity in the hydrophobic PVDF matrix that resists excessive water swelling in the hydrophilic SPS channels. This allows the application of the PEM structure with a high IEC value, without a concern for proton dilution and membrane dissolution.

Proton Conductivities. In general, the proton conductivity of the low molecular weight PVDF-g-SPS membrane is less reliable and difficult for comparison due to the weakened film integrity subsequent to high water uptake. Like most of the

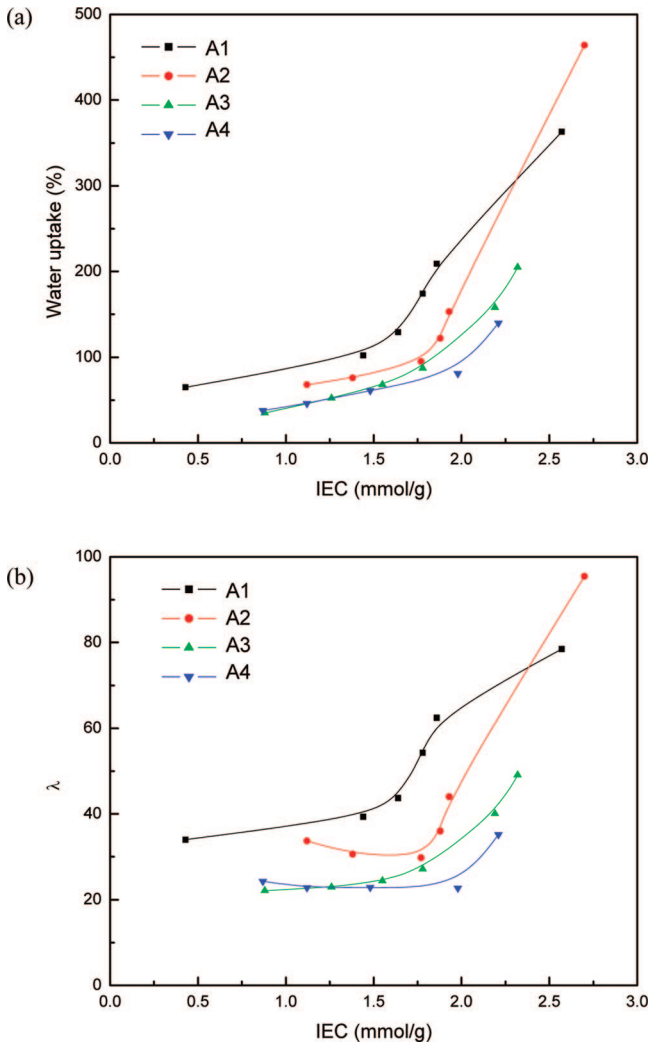

Figure 4. (a) Water uptake and (b) λ vs IEC for all low M_w PVDF-g-SPS graft copolymers (III) in Tables 1. (The lines are used solely for guiding purposes).

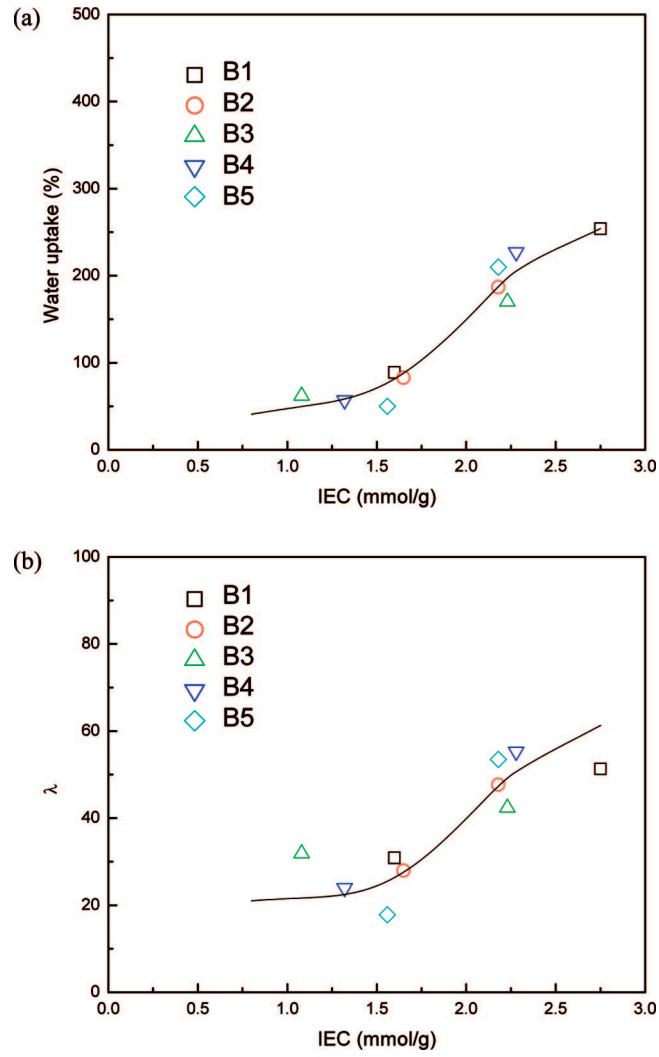

Figure 5. (a) Water uptake and (b) λ vs IEC for all high M_w PVDF-g-SPS graft copolymers (III′) in Tables 2. (The lines are used solely for guiding purposes).

PEMs, the proton conductivity of the PVDF-g-SPS graft copolymer membranes depends on the relative humidity of the environment. Figure 6 shows the plots of proton conductivity (in-plane) vs relative humidity (RH) under various environmental conditions (i.e., temperature and humidity) for the PEM based on the high molecular weight B1-2 sample. Since the graft copolymer exhibits isotropy continuous SPS ionic channels (Figure 3), it should show similar in-plane and through-plane conductivity.[24] For comparison, Nafion 112 (a random copolymer) was also measured under similar conditions.

As expected, the conductivity exponentially increases with RH, and it requires more than 60% RH to show significant proton conductivity. In the RH >60% range, the B1-2 membrane shows notably higher proton conductivity than Nafion 112 in all three measured temperatures (30, 80, and 120 °C), but Nafion 112 performs better under low RH conditions, especially at 120 °C. This conversion may be related to the water content (λ). The short-range cluster-network morphology in Nafion may be better in retaining the absorbed water molecules in PEM under high temperature and low humidity conditions. However, under high humidity conditions, the water evaporation is no long a major issue. The conductivity should directly relate to the IEC value, water content (λ), morphology, and temperature. The B1-2 graft copolymer, with the combination of high molecular weight, low graft density, and isotropic long-range hydrophilic−

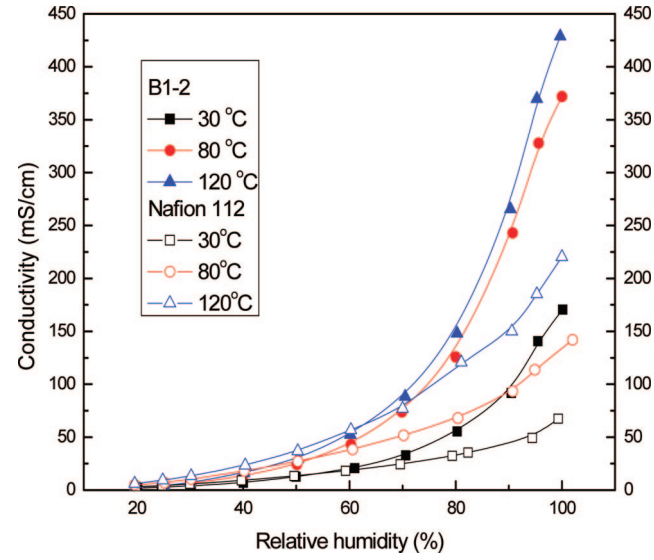

Figure 6. Comparison of proton conductivity vs relative humidity between B1-2 and Nafion 112 PEMs at 30, 80, and 120 °C. (The lines are used solely for guiding purposes).

hydrophobic phase separation, allows the incorporation of high sulfonic acid content (IEC = 2.75 mmol/g) without showing

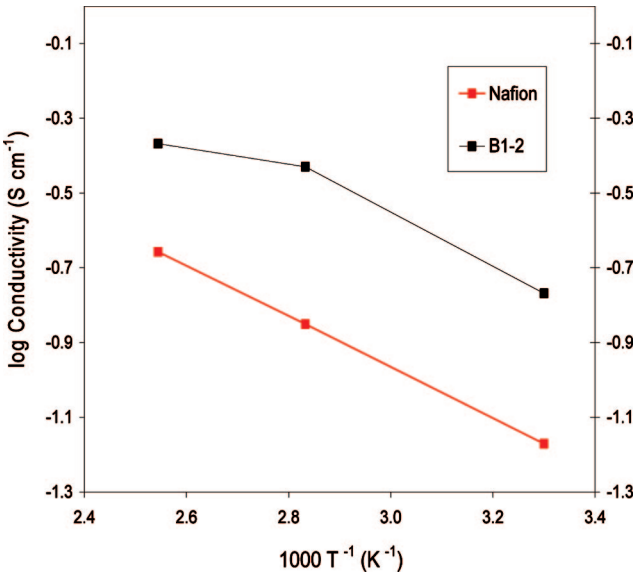

Figure 7. Comparison of proton conductivity vs temperature (1/*T*) between B1-2 and Nafion 112 at 100% relative humidity. (The lines are used solely for guiding purposes).

the negative consequence of excessive water swelling for high proton conductivity under high RH conditions.

In detail, the proton conductivity of the B1-2 PEM increases quickly as testing temperature is elevated from 30 to 80 °C, showing only an incremental increase from 80 to 120 °C. As reported,[31,32] the increase in conductivity with temperature is attributed to the activation barriers for proton motion. Once the temperature is sufficiently high to overcome the activation barrier, further increasing the temperature has much less effect on the proton conductivity. It seems that 80 °C is sufficient for sample B1-2 but not enough for Nafion 112, which still leads to increased proton conductivity after 80 °C. Figure 7 compares proton conductivity vs temperature (1/*T*) between B1-2 and Nafion 112 at 100% relative humidity. The temperature dependence can be approximated by an Arrhenius law, which yields the activation energy of 12.4 kJ mol^{-1} for Nafion 112 in the 30−120 °C temperature range and 12.9 kJ mol^{-1} and 3.9 kJ mol^{-1} for B1-2 in the temperature ranges of 30−80 °C and 80−120 °C, respectively. Similar trends are also observed in all comparative measurements under high humidity (>60%) conditions. The significant reduction of activation energy of B1-2 at high temperature range is consistent with the better continuous network of the ionic conductive channels under high humidity conditions.

In order to further understand the influence of the polymer microstructure on proton conductivity of the membrane, a series of high molecular weight PVDF-g-SPS graft copolymers (III′) with similar IEC ∼ 2.20 mmol/g and different graft densities (0.8, 1.4, 1.7, and 2.4 mol%) are compared in Figure 8. The major difference between these polymers is their microstructures, and therefore different morphologies, formed in the corresponding membranes. Proton conductivity at a low temperature (25 °C) and high humidity (80%) decreases from 120 mS/cm to 55 mS/cm when grafting density is increased from 0.8 mol% to 2.4 mol%. However, at a higher temperature (120 °C) and similar humidity (70%), a completely inverse result was observed; in this instance, the polymer with a higher graft density exhibited higher proton conductivity. A similar trend was also observed at the same high temperature (120 °C) and lower humidity (50%). Overall, in this PVDF-g-SPS graft copolymer set with the same sulfonic acid content, the lower graft density and longer graft length lead to a larger-scaled hydrophilic domain and lower activation energy. As a result,

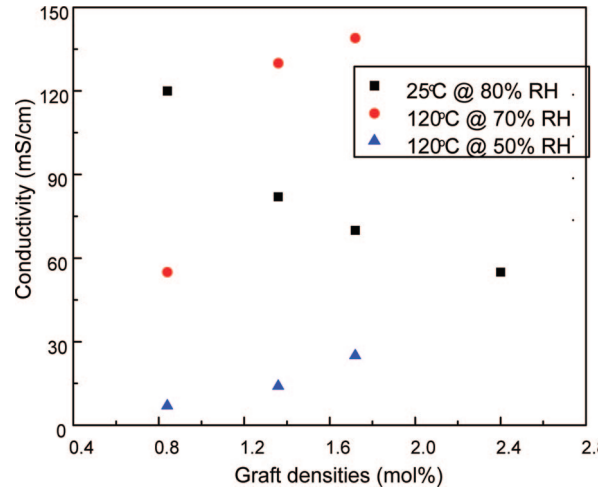

Figure 8. Comparison of proton conductivity vs graft density of four PVDF-g-SPS (III′) graft copolymers having IEC ∼ 2.20 mmol/g and different graft densities 0.8, 1.4, 1.7, and 2.4 mol%, respectively, under 25 °C (80% RH) and 120 °C (70% and 50% RH).

Table 3. Comparison of Proton Conductivity between Several Pairs of PVDF-g-SPS-Based PEMs Having Similar IEC Numbers but Different (low and high) PVDF Backbone Molecular Weight

samples	compositions (VDF/St/SSt)[a] (mole ratio)	graft[b] density (mol%)	IEC (mmol/g)	proton conductivity (mS/cm) 25 °C@80%[c]	120 °C@70%
A1-6	99.0/0.0/31.5	0.4	2.57	100	77
B1-2	94.0/0.0/36.1	0.3	2.75	150	125
A2-3	98.0/3.7/18.1	0.8	1.77	158	28
B2-1	94.0/11.1/18.3	0.8	1.65	120	55
A3-5	96.6/8.9/27.5	1.4	2.19	88	15
B3-2	94.0/3.3/26.2	1.4	2.23	82	130
A4-5	95.4/0.6/24.9	1.8	2.21	91	16
B4-2	94.0/1.5/26.6	1.7	2.28	70	139

[a] St: styrene; SSt: sulfonated styrene. [b] Number of PS grafts per 100 VDF units in the backbone. [c] Measure condition: temperature and relative humidity.

this polymer shows high conductivity at a low temperature, quickly reaches maximum conductivity at a relatively low temperature, and even starts to exhibit decreased conductivity at a higher temperature.[23] On the other hand, the corresponding graft copolymer with a higher graft density and a shorter graft length forms cluster-network morphology with higher activation energy. The proton conductivity is relatively low at low temperature and increases consistently as the temperature is elevated until it reaches a maximum at a relatively high temperature. Generally speaking, the high molecular weight PVDF-g-SPS (III′) copolymer with a high IEC value and very low graft density (0.3 and 0.8 mol%) is suitable for PEM under high RH and a wide range of temperatures, while the corresponding higher graft density (1.4 and 1.7 mol%) ones show increased conductivity at higher temperatures. However, the graft copolymer with too high of a graft density (2.4 mol%) lost most of the PVDF crystallinity, and the PEM became too soft to maintain its integrity at 120 °C.

As discussed previously, the molecular weight of the PVDF backbone in the PVDF-g-SPS plays an important role in water uptake (Figures 4 and 5) and hydrophilic channel width (Figure 3), which is directly related to proton conductivity. Table 3 compares four pairs of PVDF-g-SPS graft copolymers (III) and (III′), with similar graft density (similar morphology but different hydrophilic channel width) and an almost identical IEC value but with a different backbone molecular weight in each pair of polymers, under various conditions. At a low testing temperature, the molecular weight (M_w) shows little effect on proton

conductivity of the PEMs. The proton conductivity of low M_w samples shows even slightly higher proton conductivity than that of high M_w samples. At a high temperature, high M_w PEMs consistently show proton conductivity much higher than that of low M_w samples, especially with high graft density pairs. It is well-known that the water uptake varies with temperature, and a higher temperature usually leads to elevated water uptake[33] under high humidity conditions. The low M_w PVDF-g-SPS (III) samples, especially the ones (A3−5 and A4−5) with high graft density and low crystallinity in the PVDF matrix, may be overswelled at high temperature. As a result, the sulfonic acid concentration is significantly reduced in the enlarged PEM. On the other hand, the high M_w PEMs with stronger hydrophobic domains show better water resistance at high temperature.

Conclusions

A series of PVDF-g-SPS graft copolymers with systematically controlled microstructure (i.e., backbone molecular weight, graft density, and graft length) have been prepared and studied for PEM applications. The microstructure of the graft copolymer directly affects PEM morphology, water uptake, and proton conductivity under various conditions (i.e., temperature and humidity). The PVDF-g-SPS graft copolymer with low graft density (0.3−0.8 mol%) and long SPS graft length forms a well microphase-separated hydrophilic−hydrophobic morphology with long-range isotropic ionic channels (lamella/cylinder) imbedded in the high crystalline PVDF matrix. This morphology lowers the critical IEC value and increases water uptake and λ value. The PVDF backbone molecular weight in the hydrophobic matrix controls the width of hydrophilic conduction channels. A high molecular weight PVDF results in a smaller channel width, lower water uptake, and resistance to excessive water swelling at a high IEC value. Although the morphology with long-range hydrophilic channels is favorable for proton conductivity with low activation energy, it also leads to high sensitivity to humidity, requiring a high RH to achieve high conductivity. In contrast, the moderately high graft density (1.4−2.4 mol%) PVDF-g-SPS graft copolymers show dispersed cluster-network morphology with a small cluster diameter, similar to that of Nafion, which is less sensitive to humidity and exhibits a smaller water uptake and λ value. The proton conductivity is still proportional to humidity warranted by the smaller slope, and the higher activation energy results in a linear increase of proton conductivity with temperature, under the same RH condition. The PVDF-g-SPS graft copolymer with a high graft density (>2.5 mol%), losing most of its crystallinity, exhibits instability (softness) at a high temperature and also exhibits excessive water swelling with a high IEC value. Generally speaking, the high molecular weight PVDF-g-SPS copolymer with low graft density and a high IEC value is suitable for PEM under a high RH and a wide range of temperatures, while the corresponding higher graft density ones show increased conductivity at higher temperatures.

Acknowledgment. The authors gratefully acknowledge the financial support of this work by the U.S. Department of Energy (Contracts #DE-FG36-06GO16036) and the donation of the high molecular weight VDF/CTFE copolymer from Solvay Solexis, Inc.

Supporting Information Available: GPC curves of VDF/CTFE copolymers, NMR spectra and TGA analysis of PVDF-g-PS and PVDF-g-SPS graft copolymers, and proton conductivity semi-log plots of PVDF-g-SPS graft copolymer. This material is available free of charge via the Internet at http://pubs.acs.org.

References and Notes

(1) Rikukawa, M.; Sanui, K. *Prog. Polym. Sci.* **2000**, *25*, 1463.
(2) Brandon, N. P.; Skinner, S.; Steele, B. C. H. *Annu. Rev. Mater. Res.* **2003**, *33*, 183.
(3) Hickner, M. A.; Ghassemi, H.; Kim, Y. S.; Einsla, B. R.; McGrath, G. E. *Chem. Rev.* **2004**, *104*, 4587.
(4) Li, Q.; He, R.; Jensen, J. O.; Bjerrum, N. J. *Chem. Mater.* **2003**, *15*, 4896.
(5) Zhou, Z.; Dominey, R. N.; Rolland, J. P.; Maynor, B. W.; Pandya, A. A.; DeSimone, J. M. *J. Am. Chem. Soc.* **2006**, *128*, 12963.
(6) Grot, W. G. (E. I. DuPont) US Patent 4,433,082, **1984**.
(7) Savadogo, O. *J. New. Mater. Electrochem. Syst.* **1998**, *1*, 47.
(8) Gottesfeld, S.; Zawodzinski, T. A. In *Advances in Electrochemical Science and Engineering*; Alkire, R. C., Gerischer, H., Kolb, D. M., Tobias, C. W., Eds.; Wiley: New York, 2002; Vol. *5*.
(9) Wainright, J. S.; Wang, J.-T.; Weng, D.; Savinell, R. F.; Litt, M. *J. Electrochem. Soc.* **1995**, *142*, L121.
(10) Wang, F.; Hickner, M.; Ji, Q.; Harrison, W.; Mecham, J.; Zawodzinski, T. A.; McGrath, J. E. *Macromol. Symp.* **2001**, *175*, 387.
(11) Asano, N.; Aoki, M.; Suzuki, S.; Miyatake, K.; Uchida, H.; Watanabe, M. *J. Am. Chem. Soc.* **2006**, *128*, 1762.
(12) Wainright, J. S.; Wang, J. T.; Weng, D.; Savinell, R. F.; Litt, M. *J. Electrochem. Soc.* **1995**, *142*, L121.
(13) Zhang, J. L.; Tang, Y. G.; Song, C. J.; Zhang, J. J. *J. Power Sources* **2007**, *172*, 163.
(14) Wiley, R. H.; Venkatachalam, T. K. *J. Polym. Sci., Part A* **1966**, *4*, 1892.
(15) Gupta, B.; Scherer, G. G. *J. Appl. Polym. Sci.* **1993**, *50*, 2129.
(16) Flint, S. D.; Slade, R. C. T. *Solid State Ionics* **1997**, *97*, 299.
(17) Hietala, S.; Koel, M.; Skou, E.; Elomaa, M.; Sundholm, F. *J. Mater. Chem.* **1998**, *8*, 1127.
(18) Torkkeli, M.; Serimaa, R.; Etelaniemi, V.; Toivola, M.; Jokela, K.; Paronen, M.; Sundholm, F. *J. Polym. Sci., Part B* **2000**, *38*, 1734.
(19) Kuhn, H.; Gubler, L.; Schmidt, T. J.; Scherer, G. G.; Brack, H. P.; Simbek, K.; Rager, T.; Geiger, F. Proceedings of the 2nd European PEFC Forum; European Fuel Cell Forum: Switzerland, 2003; p 69.
(20) Shi, Z. Q.; Holdcroft, S. *Macromolecules* **2004**, *37*, 2084.
(21) Zhang, M. F.; Russell, T. P. *Macromolecules* **2006**, *39*, 3531.
(22) Shi, Z. Q.; Holdcroft, S. *Macromolecules* **2005**, *38*, 4193.
(23) Xu, K.; Li, K.; Khanchaitit, P.; Wang, Q. *Chem. Mater.* **2007**, *19*, 5937.
(24) Tsang, E. M. W.; Zhang, Z. B.; Shi, Z. Q.; Soboleva, T.; Holdcroft, S. *J. Am. Chem. Soc.* **2007**, *129*, 15106.
(25) Milner, S. T. *Macromolecules* **1994**, *27*, 2333.
(26) Xenidou, M.; Beyer, F. L.; Hadjichristidis, N.; Gido, S. P.; Tan, N. B. *Macromolecules* **1998**, *31*, 7659.
(27) Zhang, Z. C.; Chung, T. C. M. *Macromolecules* **2006**, *39*, 5187.
(28) Chung, T. C.; Petchsuk, A. *Macromolecules* **2002**, *35*, 7678.
(29) Wang, Z. M.; Zhang, Z. C.; Chung, T. C. M. *Macromolecules* **2006**, *39*, 4268.
(30) Veriss, R. A.; Sen, A.; Willis, C. L.; Pottick, L. A. *Polymer* **1991**, *32*, 1867.
(31) Damay, F.; Klein, L. C. *Solid State Ionics* **2003**, *162−163*, 261.
(32) Alberti, G.; Casciola, M.; Massinelli, L. Bauer, B. *J. Membr. Sci.* **2001**, *185*, 73.
(33) Zhou, Z. L.; Dominey, R. N.; Rolland, J. P.; Maynor, B. W.; Pandya, A. A.; DeSimone, J. M. *J. Am. Chem. Soc.* **2006**, *128*, 12963.

MA801277M